

MIXED-MODE THROUGH-THICKNESS FRACTURE OF POLYMER MATRIX COMPOSITES

J. Jamali, J.T. Wood*

Mechanical and Materials Engineering Department, Western University, London, Canada

* Corresponding author (jtwood@uwo.ca)

Keywords: *Mixed mode, through-thickness-fracture, PMC*

Abstract

Through thickness fracture behaviour of unidirectional (UD) glass fibre epoxy and neat epoxy under various in-plane loading is studied. A model is proposed to characterize the toughness of UD composite based only on the constituents and interfacial properties. Loading from pure mode I, pure mode II, and different mixed mode I/II ratios were applied to the specimen using a compact tension shear (CTS) fixture.

1 Introduction

Materials are properly chosen for engineering applications based on their mechanical or physical properties, including mass, strength, stiffness, and toughness. The ability to exploit the lightweight potential of fibre-reinforced polymer composites is dependent, in many applications, on the ability to predict their fracture behaviour. Furthermore, high-volume manufacturing processes (e.g. those suitable for automotive applications) based on compression molding techniques typically result in planar random arrays of discontinuous fibres. Thus, an advancing through-thickness crack will meet transverse fibres at a range of angles between 0° and 90°. In this research, the propagation of a through-thickness crack in a UD composite was studied as a function of loading angle with respect to the macroscopic initial crack direction using the CTS test geometry in order to assess the associated crack propagation energy.

2 Background

In the study of composite fracture, it is necessary to discern between interlaminar fracture and through-thickness fracture, because an advancing crack will see a different arrangement of fibres in each case. Interlaminar fracture can be characterized by test methods like Double Cantilever Beam (DCB) and

the End Notched Flexure (ENF) for mode I and II, respectively [1] and [2]. For mixed mode fracture properties, beam type specimens are used most often [3].

The specimen geometries used for interlaminar fracture studies are often not appropriate for through-thickness measurements because the fibres in the specimens are generally oriented in the plane of the sheet.

The CTS sample has the advantage that the width of the crack is oriented in the thickness direction of the composite panel. This test method also has the advantage that a single specimen geometry can be used to study all modes of loading.

The CTS specimen was introduced in the literature to study mixed mode loading on homogenous materials like aluminum [4]. The specimen was later developed to be used to study interlaminar fracture behaviour of composite materials [5].

3 Failure Model

An energy based failure model is proposed here. The model predicts the value of critical strain energy release rate (CSERR) of a UD polymer composite based on the fracture properties of its constituents. The properties required to find CSERR of the composite include resin mode I and mode II CSERR, and fibre/matrix interfacial CSERR.

To begin, we consider a UD composite in which the fibre orientation is parallel to the notch direction of the CTS specimen geometry shown in Fig.1. The specimen is subjected to a far field stress, σ , applied at an angle, α , to the specimen axis. This applied stress, σ , can be resolved into the normal and shear components, σ_y , and τ_{xy} , as shown in Fig.1. For the geometry of Fig.1:

$$\sigma_y = \sigma \cos \alpha \quad (1)$$

$$\tau_{xy} = \sigma \sin \alpha \quad (2)$$

The mode I and mode II stress intensity factors, K_I and K_{II} at the tip of the crack can be expressed as:

$$K_I = Y_1 \sigma_y \sqrt{\pi a} \quad (3)$$

$$K_{II} = Y_2 \tau_{xy} \sqrt{\pi a} \quad (4)$$

where, Y_1 and Y_2 are dimensionless geometry components that depend on crack length, a , and width of the specimen, w . The values of K_I and K_{II} for CTS specimen are found using the following relations [6] and [7]:

$$K_I = \frac{P\sqrt{\pi a} \cos \alpha}{wt \left(1 - \frac{a}{w}\right)} \sqrt{\frac{0.26 + 2.65 \left(\frac{a}{w-a}\right)}{1 + 0.55 \left(\frac{a}{w-a}\right) - 0.08 \left(\frac{a}{w-a}\right)^2}} \quad (5)$$

$$K_{II} = \frac{P\sqrt{\pi a} \sin \alpha}{wt \left(1 - \frac{a}{w}\right)} \sqrt{\frac{-0.23 + 1.4 \left(\frac{a}{w-a}\right)}{1 - 0.67 \left(\frac{a}{w-a}\right) + 2.08 \left(\frac{a}{w-a}\right)^2}} \quad (6)$$

where P , is the critical (maximum) load corresponding to the crack opening, t is the specimen thickness and a is the crack length.

Using Equations 1 and 2, the stress intensity factors can be restated as:

$$K_I = Y_1 \sigma \cos \alpha \sqrt{\pi a} \quad (7)$$

$$K_{II} = Y_2 \sigma \sin \alpha \sqrt{\pi a} \quad (8)$$

Defining the effective value of stress intensity factor as:

$$K_{eff} = \sqrt{K_I^2 + K_{II}^2} \quad (9)$$

The CSERR can then be expressed as a function of α (assuming plane strain):

$$G_c = K_{eff}^2 \frac{1 - \nu^2}{E} = \frac{(K_I^2 + K_{II}^2)(1 - \nu^2)}{E} \quad (10)$$

Substituting Equations 7 and 8 into Equation 10 gives:

$$G_c = \cos^2 \alpha Y_1^2 \sigma^2 \frac{\pi a (1 - \nu^2)}{E} + \sin^2 \alpha Y_2^2 \sigma^2 \frac{\pi a (1 - \nu^2)}{E} \quad (11)$$

or

$$G_c = \cos^2 \alpha \frac{K_{Ic}^2 (1 - \nu^2)}{E} + \sin^2 \alpha \frac{K_{IIc}^2 (1 - \nu^2)}{E} \quad (12)$$

since [8]:

$$G_{Ic} = \frac{K_{Ic}^2 (1 - \nu^2)}{E} \quad (13)$$

$$G_{IIc} = \frac{K_{IIc}^2 (1 - \nu^2)}{E} \quad (14)$$

Therefore, Equation 12 can be written as:

$$G_c = \cos^2 \alpha G_{Ic} + \sin^2 \alpha G_{IIc} \quad (15)$$

Equation 15 states that the CSERR for any material in which the crack propagates parallel to the original notch, can be determined with the knowledge of the values of mode I and mode II CSERR. Equation 15 results in the prediction of toughness as a function of a loading angle with the general form shown in Fig. 2.

Equations 13 and 14 can be used for an isotropic material like epoxy. When the material is anisotropic, the relations that are used to find the value of the toughness should consider other elastic parameters of the material, [9] and [10]. Therefore, the relation between CSERR and fracture toughness can be written as:

$$G_I = K_I^2 \sqrt{\frac{\bar{S}_{11} \bar{S}_{22}}{2}} \left[\sqrt{\left(\frac{\bar{S}_{11}}{\bar{S}_{22}}\right)} + \frac{2\bar{S}_{12} + \bar{S}_{66}}{2\bar{S}_{11}} \right]^{\frac{1}{2}} \quad (16)$$

$$G_{II} = K_{II}^2 \frac{\bar{S}_{11}}{\sqrt{2}} \left[\sqrt{\left(\frac{\bar{S}_{11}}{\bar{S}_{22}}\right)} + \frac{2\bar{S}_{12} + \bar{S}_{66}}{2\bar{S}_{11}} \right]^{\frac{1}{2}} \quad (17)$$

where \bar{S}_{ij} are elements of transformed compliance tensor, $[\bar{S}]$, which is defined as:

$$[\bar{S}] = [T']^{-1} [S] [T] \quad (18)$$

and

$$[T']^{-1} = \begin{bmatrix} \cos^2 \theta & \sin^2 \theta & -\cos \theta \cdot \sin \theta \\ \sin^2 \theta & \cos^2 \theta & \cos \theta \cdot \sin \theta \\ 2\cos \theta \cdot \sin \theta & -2\cos \theta \cdot \sin \theta & \cos^2 \theta - \sin^2 \theta \end{bmatrix} \quad (19)$$

The angle θ (Fig. 5) is the fibre angle which is equal to 90° for a UD composite in which the fibre orientation is parallel to the notch direction of the CTS specimen, and matrix S is the compliance tensor of the composite [11].

Determining Toughness

It now remains to determine the critical values of G_I and G_{II} . Since the goal is to be able to develop a predictive model based only on the properties of the constituents, it is useful to recognize that mode I and mode II toughness are the summation of the toughness of each of the constituents represented on the fracture surface. i.e.:

MIXED-MODE THROUGH-THICKNESS FRACTURE OF POLYMER MATRIX COMPOSITES

$$G_{Ic} = G_{Ic,i} \frac{A_i}{A_t} + G_{Ic,m} \frac{A_m}{A_t} + G_{Ic,f} \frac{A_f}{A_t} \quad (20)$$

$$G_{IIc} = G_{IIc,i} \frac{A_i}{A_t} + G_{IIc,m} \frac{A_m}{A_t} + G_{IIc,f} \frac{A_f}{A_t} \quad (21)$$

where the subscripts i , m , f , indicate the interface, matrix, and fibre respectively. A_m , A_i , A_f , and A_t are the matrix, interface, fibre and total area of the fracture surface respectively (Fig. 3).

The values of A_m , A_i , A_t can be estimated from the fibre volume fraction of the composite. For example, we have the following relation for square array (Fig.3) and hexagonal array of fibres inside the matrix respectively [11]:

$$m = 2r \left[\sqrt{\frac{\pi}{4f}} - 1 \right] \quad (22)$$

$$m = 2r \left[\left(\frac{\pi}{2f\sqrt{3}} \right)^{\frac{1}{2}} - 1 \right]$$

where r is the fibre radius, m is the spacing between fibres, and f is the fibre volume fraction as shown in the square arrayed fibres in Fig. 3.

The values of interface and matrix area for each unit cell at the fracture surface can be found as:

$$\begin{aligned} A_i &= \pi \cdot r \cdot l \\ A_m &= m \cdot l \\ A_t &= (m + 2r)l \end{aligned} \quad (23)$$

where l is the length of the fracture surface as shown in Fig.3. It is important to recognize that because of the curvature of the interfacial area, the sum of A_i , and A_m , will be greater than the total projected area, A_t .

For the materials studied here, the crack is known to propagate along the fibres, and thus the projected area of fibre on the fracture surface, A_f , will be zero.

Therefore, Equations 14 and 15 simplify to:

$$G_{Ic} = G_{Ic,i} \frac{A_i}{A_t} + G_{Ic,m} \frac{A_m}{A_t} \quad (24)$$

$$G_{IIc} = G_{IIc,i} \frac{A_i}{A_t} + G_{IIc,m} \frac{A_m}{A_t} \quad (25)$$

The theory presented in the preceding sections suggests that it should be possible to predict the CSERR of a UD composite loaded at any angle with respect to the notch, based on knowledge of the toughness of the matrix, the fibre, and the interface between them. It now remains to measure these values.

4 Experimental Method

4.1 Materials and Manufacturing

For this study, UD E-glass and epoxy material (CLR1180/CLH6560 manufactured by Crosslink Tech. Inc.) were utilized.

Composite panels were manufactured by the hand lay-up of 12 layers of UD glass fibre to give the required thickness for the test. The resin is then cured at 60°C for 4 hours under a hydraulic hot press. The pressure can be altered to give different thicknesses and fibre volume fraction for the composite. In order to keep the value of volume fraction in the sample consistent, the pressure is fixed at 25psi on the UD layers.

The neat epoxy sample in this study is made using the same epoxy as UD composite with a similar mixing procedure (here 100 units of resin with 30 units of Hardener). The mixed resin is then poured into trays that were lined by vacuum bags to avoid resin adhering to the trays. The trays were leveled to give even value of thickness in the resin sheet and then cured at room temperature for 48 hours.

Both neat epoxy and UD composite were then cut to the required dimension using a milling machine.

4.2 Richards Test

In this study we investigate the mixed mode response of the unreinforced epoxy as well as the mixed mode response of UD composite using the CTS test. The CTS test setting and CTS specimen geometry are shown in Fig. 4 and Fig. 5. The load is applied to the CTS specimen using a fixture made of steel. The steel fixture has lower and upper grips which were fixed at grips of the testing machine and then the specimen is fixed to the grips using 6 steel bolts. By adjusting the pin location on the fixture, different angles between $\alpha = 0^\circ$ (mode I) and $\alpha = 90^\circ$ (mode II) were generated in the specimen. Angles between 0° and 90° correspond to mixed mode loading (Fig. 4).

The CTS specimen has a notch size equal to half of its width (the crack length is suggested to be between $0.45w$ and $0.7w$ [4]). As shown in Fig. 5, the CTS Specimen has a pre-crack of approximately 0.5mm long cut into the artificial crack tip using a razor blade.

The testing is performed using an Instron servohydraulic load frame (Instron 8804). The load is measured by 250kN or 5kN load cell depending on the range of the load required for the test. The displacement rate is 2mm/min and the test is performed at room temperature.

The maximum load at which the crack opens up is measured and used for the calculation of the mode I, K_{Ic} , and mode II, K_{IIc} , the fracture toughness of the composite.

After fracture testing, the fracture surface is carefully cut at a low rate and stored away from humidity to reduce post-failure damage [12]. The surface is then studied using scanning electron microscopy to observe the constituents on the fracture surface. The fibre volume fractions of the samples were then measured by a burn-off test at 560°C for 1 hour according to ASTM D2584. The fibre volume fraction of the UD samples is between 40% and 50% [13].

4.3 Notch Sensitivity

To assess the influence of the notch geometry on the fracture response of material, an additional study was performed with different shaped notches. A series of tests on UD composites were carried out that had a U-notch (2.5mm radius), a 45° V-notch, and a V-notch with a slit made by a razor blade.

The study of the notch shape on neat epoxy showed that the fracture behaviour of the epoxy is affected by the shape of the notch, while the effect of the notch shape in a UD composite was not observed to be significant on the fracture load. As the crack opening in a UD composite occurs due to interfacial failure, the bonding between the fibre and matrix is the critical parameter, and not the shape of the notch. Therefore, a V-shape notch could be used for all composite specimens.

4.4 Specimen Gripping Bolt Hole Failure

For some combinations of fibre orientation and loading angle, it was found that the specimens would fracture at the bolt holes, rather than at the notch tip as shown in Fig. 6. These failures were attributed to the weakness of the UD composite in the transverse direction, combined with the stress concentration at the bolt holes. This problem was addressed by adding a satin scrim layer to the outer surfaces of the specimens during the manufacturing process, and by incorporating 180 grit sandpaper between the steel fixture and the specimen.

4.5 Data Analysis

Mode I and mode II fracture toughness, K_{Ic} and K_{IIc} , of the composite is calculated using the maximum load, P , at which the crack opens up during the CTS

test. Fracture toughness values are calculated using Equations 5 and 6.

The values of K_{Ic} and K_{IIc} were then used to find mode I and mode II CSERR, using Equations 16 and 17 for the composite.

In order to use Equations 24 and 25, the mode I and II CSERR for the interface and resin can be found from mode I and II testing of transverse composite and neat epoxy respectively.

5 Results and Discussion

5.1 Neat Epoxy

Epoxy specimens were tested to find the values of mode I, mode II and mixed mode CSERR. CTS specimens were used for finding mode I CSERR. The values measured for epoxy were different from those found in literature, therefore, thicker samples were made and tested using a single notch edge beam test according to ASTM 5045 [14].

5.1.1 Effect of Specimen Thickness

Critical value for fracture toughness is found when the material is in the plane strain condition. Therefore, a larger thickness is required to reach the plane strain state in a material. Thicker samples have a smaller region experiencing plastic deformation resulting in a smaller value of toughness compared to thinner samples [8]. Therefore, the effect of thickness was studied on the value of fracture toughness of epoxy samples. The results are shown in Fig.7a. The figure shows that a minimum thickness of 11mm is required to ensure a state of plane strain to measure the correct value for mode I fracture toughness.

The value measured for mode I fracture toughness and mode I CSERR are $3.07 \text{ MPa}\sqrt{\text{m}}$ and $3.2 \frac{\text{KJ}}{\text{m}^2}$ respectively.

Mode II fracture toughness and CSERR using CTS samples were measured as $K_{IIc} = 4.89 \text{ MPa}\sqrt{\text{m}}$ and $G_{IIc} = 7.05 \text{ KJ/m}^2$.

The mixed mode experiments on the epoxy specimens showed that P_{max} increased as the loading angle increased (Fig. 7b).

Specimens fracture under mode I at the notch tip, as the crack propagates in a 0° direction (parallel to the notch direction). The propagation angle varies from 0° to 75° for mixed mode ratios between mode I and mode II. For some of mode II samples macro hackles were observed. Multiple macro hackles were observed in the broken samples, starting from a few

MIXED-MODE THROUGH-THICKNESS FRACTURE OF POLYMER MATRIX COMPOSITES

millimeters away from the tip of the crack as shown in Fig. 8.

Effective values of fracture toughness, K_{eff} , and CSERR, G_c , vs. the loading angle for epoxy are shown in Fig. 7c and 7d.

Fig. 7d also shows how well the failure model (Equation 15) can predict the fracture behaviour under a mixed mode of loading.

5.2 UD Composite

We cannot measure interfacial toughness directly but we can measure G_I and G_{II} of the composite in order to infer the values of interfacial toughness.

The value measured for mode I fracture toughness and mode I CSERR are $3.7 MPa\sqrt{m}$ and $1.02 \frac{KJ}{m^2}$ respectively.

Mode II fracture toughness and CSERR using CTS samples were measured, which give $K_{IIc} = 4.9 MPa\sqrt{m}$ and $G_{IIc} = 4.62 KJ/m^2$.

The values of fracture toughness match with the literature [15]. The values of mechanical properties of the UD composite used in the calculations are given in Table 1.

Fracture behaviour of a composite over the entire range of loading angles, showed that the crack in the sample initiated at the notch tip and then propagated along the fibre/matrix interface. Thus, for loading angles other than 0° and 90° , the cracks propagate under mixed mode loading conditions. When the load is applied to the composite, a white image on the path of crack is observed before the load reaches maximum. This white image represents the existence of tiny micro-cracks at the fibre matrix interface due to the load. At maximum load, P_{max} , these micro-cracks come together and make a visible crack at the tip of the notch in the fibre direction. The process of crack propagation is faster for thicker samples than thinner ones.

The displacement at the peak load decreases from 90° loading angle to 0° loading angle. The drop in failure displacement results in a lower value of energy absorption and toughness in a UD composite with smaller loading angles. Therefore, the values of CSERR rise from $1.02 \frac{KJ}{m^2}$ for mode I to $4.62 \frac{KJ}{m^2}$ for mode II as shown in Fig. 9.

Fracture surfaces of broken samples were characterized using Scanning Electron Microscopy (SEM). On the fracture surface, interfacial debonding, fibre pull out and matrix plastic fracture were observed (Fig. 10). Due to the hinge effect at the tip of the crack and rotation of crack mouth during the

test at angles close to 0° some fibres are pulled out or were broken (Fig. 11)

5.3 Interfacial Toughness

After measuring the values of $G_{Ic} = 1.02 kJ/m^2$, $\frac{A_i}{A_t} = 1.16$, $\frac{A_m}{A_t} = 0.26$ and $G_{Ic,m} = 3.2 kJ/M^2$ if Equation 24 is used to find the interfacial CSERR, it gives a negative value for $G_{Ic,i}$ which is meaningless. Therefore, Equation 24 should be modified.

For modifying Equation 24 we know that the energy released under mode I in the composite is the summation of energy released in the matrix and interface. The major part of the energy dissipated in the matrix during crack propagation is due to plastic deformation at the tip of the crack. The plastic region has a plastic radius which is calculated using [8]:

$$r_p = \frac{1}{3\pi} \left(\frac{K_I}{\sigma_{y,p}} \right)^2 \quad (26)$$

which gives a radius of 434mm for epoxy. As the matrix is reinforced by the fibre, the size of the plastic zone is limited to the fibre spacing. For FVF=0.43, the fibre spacing is 5.3micron comparing to 434micron calculated from Equation 26. Therefore, the contribution of the matrix plastic deformation to the value of CSERR will be much smaller, and Equation 24 should be modified to:

$$G_{Ic} = G_{Ic,i} \frac{A_i}{A_t} + \eta \cdot G_{Ic,m} \frac{A_m}{A_t} \quad (27)$$

where η is a reinforcement reduction factor. This value is 0.012 which gives $G_{Ic,i}$ to be $989 \frac{J}{m^2}$ which agree with [16].

5.4 The Failure Model (Prediction of G)

Mode I, mode II and mixed mode loading was applied to transverse UD composites.

The results for the failure model using Equation 8 and experimental results of 90° UD composite under different modes of loading (different α) are compared in Fig. 12.

In comparison with experimental results for off-axis loading as can be seen in Fig. 12, the model can predict the value of energy release rate in a composite quite well. The discrepancy of experimental results, especially for high percentages of mode II, can be due to variability in experimental materials such as differences in fibre orientation and fibre volume fraction during the hand lay up of

composites. The continuous polymer threads that keep the UD fibres together could also affect the value of fracture work (Fig. 13). Another important aspect that can affect the fracture work could be fibre pull out and fibre friction during mode II of loading.

Based on the observations, this research paper reports the following items:

- K and G are reported for neat epoxy as a function of a loading angle.
- K_{eff} and G_{eff} are also reported as a function of a loading angle.

A model is proposed to characterize the toughness of UD composite based only on the constituents and interfacial properties.

Conclusions

- The model has been shown to work well for UD composites, where the notch is parallel to the fibre direction
- This work will be extended to consider the case of other fibre orientations with the goal to eventually predict the toughness of random fibre orientations

Future Work

Based on the approach discussed to predict the fracture properties of UD composites, similar methods can be used for the prediction of fracture properties of random fibre composites. The crack in random composites meets fibres in different directions. The hypothesis is if there are more fibres aligned in a certain direction, the crack advances in that direction, and after a few millimeters of propagation if the fibres are aligned in the other direction the direction is changed. For a random composite the crack path is expected to behave like isotropic material with a zigzag pattern in the fracture surface including fibre pull out, fibre matrix and interface fracture.

References:

- [1] M. Kanninen, "An augmented double cantilever beam model for studying crack propagation and arrest," *International Journal of Fracture*, 1973.
- [2] J. G. LA Carlsson, "On the analysis and design of the end notched flexure (ENF) specimen for mode II testing," *Journal of Composite Materials*, 1986.
- [3] A. D6671/D6671M-06, "Standard Test Method for Mixed Mode I-Mode II Interlaminar Fracture Toughness of Unidirectional Fiber Reinforced Polymer Matrix Composites," ASTM, 2006.
- [4] H. A. Richard and K. Benitz, "A loading device for the creation of mixed mode in fracture mechanics," *International Journal Of Fracture*, 1983.
- [5] Rikards, Buchholz and H. A. Richard, "Investigation of mixed mode I/II interlaminar fracture toughness of laminated composites by using a CTS type specimen," *Eng. Fracture Mechanics*, pp. 325-342, 1998.
- [6] H. Richard, "Some theoretical and experimental aspects of mixed mode fractures," *Advances in Fracture Research*, pp. 3337-3344, 1984.
- [7] K. Hashimoto, "On Consideration for Fracture Toughness Evaluation of Mode II," *Research report of the Tokuyama technical college*, pp. 31-35, 2007.
- [8] D. Broek, *Elementary engineering fracture mechanics*, Martinus Nijhoff publishers, 1982.
- [9] GC Sih, PC Paris, GR Irwin, "On cracks in rectilinearly anisotropic bodies," *International Journal of Fracture Mechanics*, 1965.
- [10] Parhizgar S., Zachary L., Sun C.T., "Application of the principles of linear fracture mechanics to the composite materials," *International journal of fracture*, vol. 20, pp. 3-15, 1982.
- [11] D. Hull and T. W. Clyne, *An introduction to composite materials*, Cambridge university press, 1996.
- [12] E. Greenhalgh, *Failure analysis and fractography of polymer composites*, CRC press, 2009.
- [13] A. D2584, "Standard Test Method for Ignition Loss of Cured Reinforced Resins," in *ASTM*, 2008.
- [14] "Standard Test Methods for Plane-Strain Fracture Toughness and Strain Energy Release Rate of Plastic Materials," in *ASTM 5045*, ASTM, 2007.
- [15] *Cambridge Engineering Selector (CES)*, Granata Design Limited.
- [16] Detassis M, Frydman E, Vrieling D, Zhou X-F, Wagner HD, Nairn JA, "Interface Toughness in Fiber Composites by the Fragmentation Test," *Composites Part A: Applied Science and Manufacturing*, vol. 27, pp. 769-773, 1996.

MIXED-MODE THROUGH-THICKNESS FRACTURE OF POLYMER MATRIX COMPOSITES

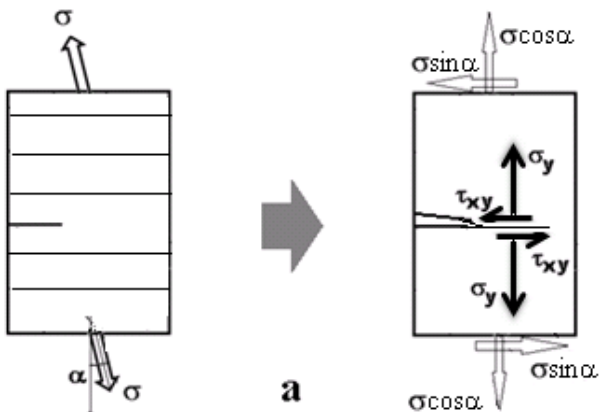


Fig. 1. General state of stress at the elements shown in the CTS sample for a mixed mode I and II and crack propagation along the interface under mixed mode loading.

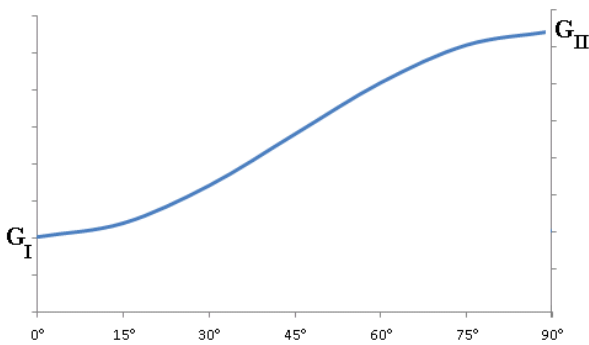


Fig.2. The mixed mode toughness pattern predicted for different modes of loading.

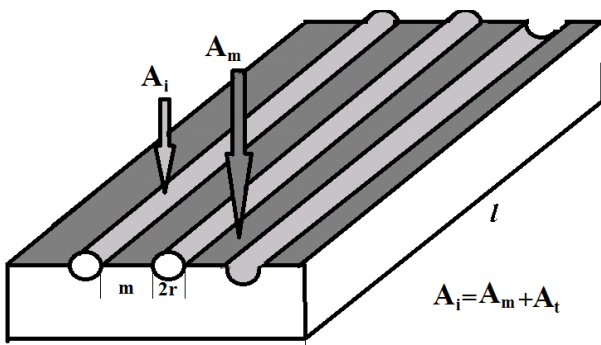


Fig.3. Schematic fracture surface morphology and corresponding values of the matrix and interface fracture area.

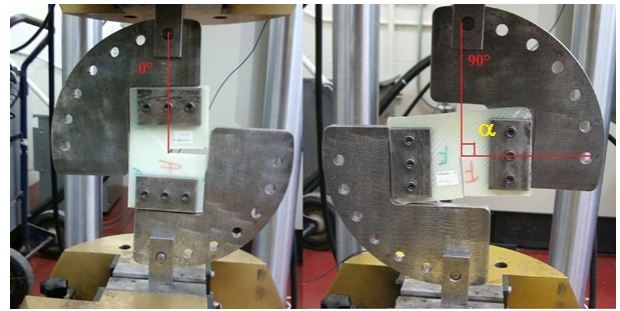


Fig. 4. CTS fixture. Left) mode I. Right) mode II.

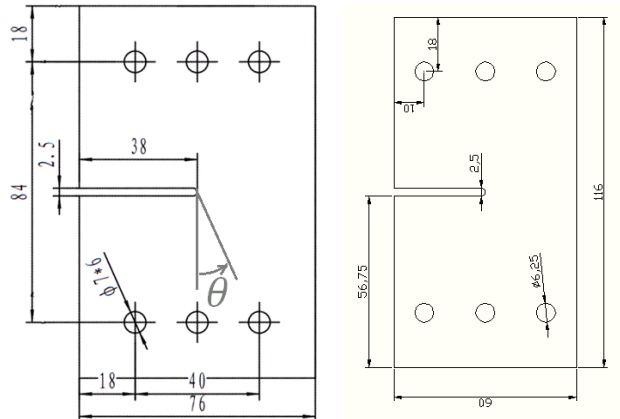


Fig. 5. CTS sample, fibre angle denoted by θ (left). Neat epoxy specimen (right)

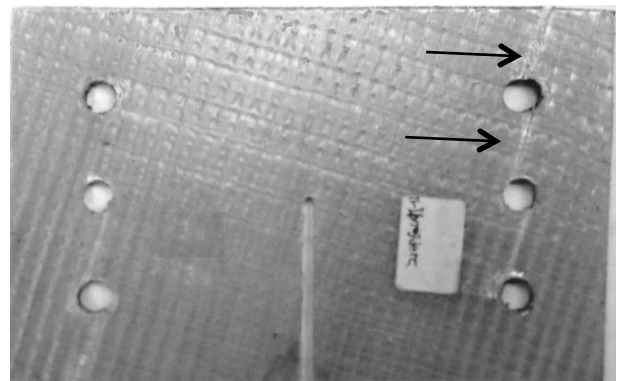
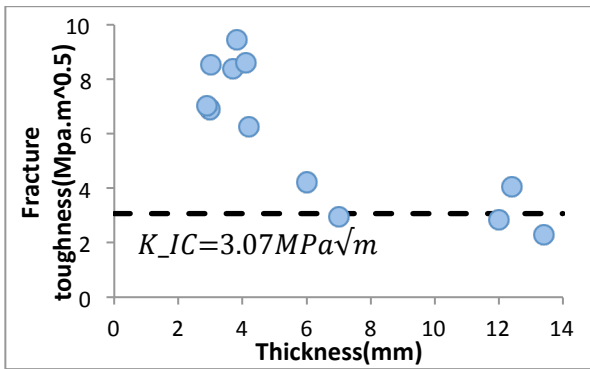
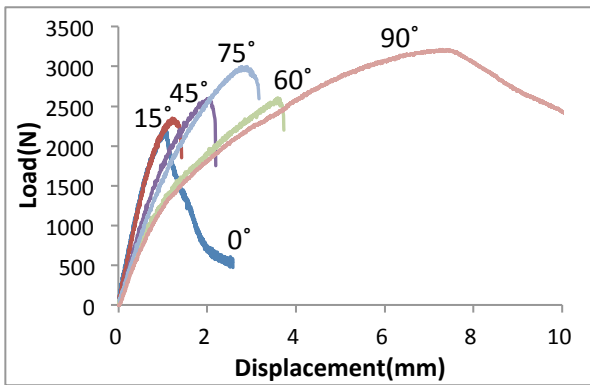


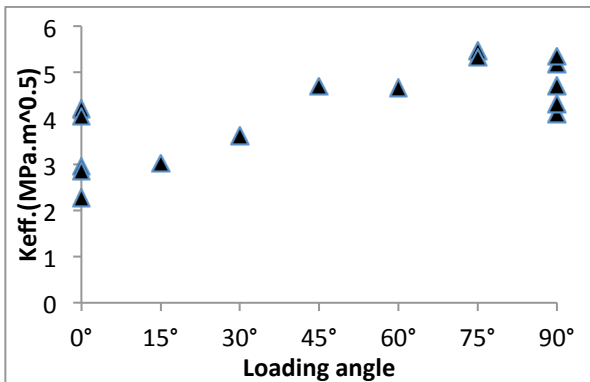
Fig. 6. Examples of bolt hole failure in 90 ° and 75° UD composite specimen under mode II loading. No notch opening is observed at the sample and the results are not good for the calculation of fracture properties.



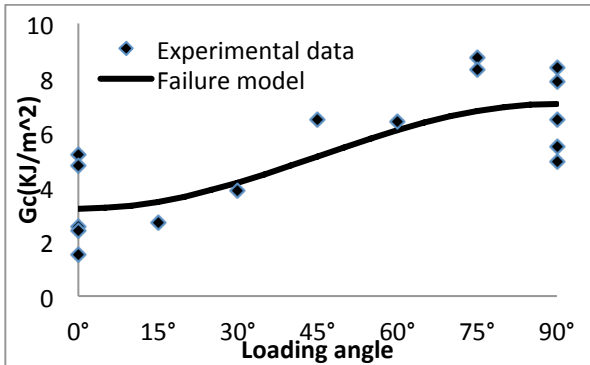
a



b



c



d

Fig. 7a) thickness effect on mode I fracture toughness

b) epoxy load-displacement, sample thicknesses between 3 and 4mm.

c) effective fracture toughness vs. loading angle
d) toughness vs. loading angle.

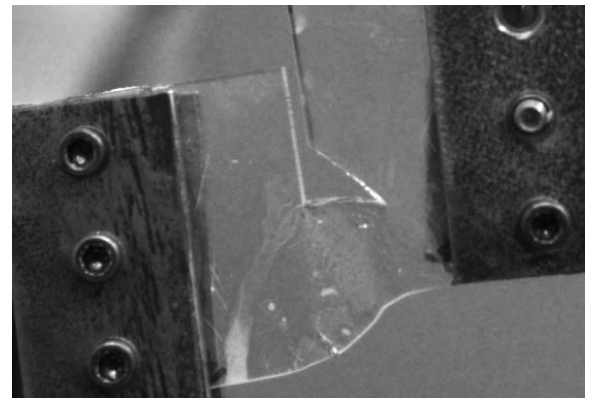
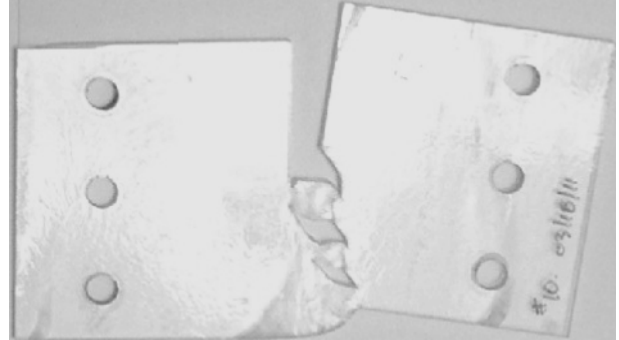


Fig. 8. Macro hackles in some of neat epoxy specimen under mode II loading, sample with macro hackle (top) sample without macro hackling (bottom).

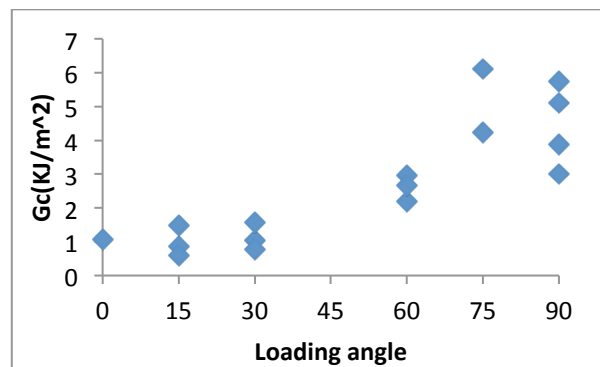


Fig. 9. UD composite toughness vs. loading angle

MIXED-MODE THROUGH-THICKNESS FRACTURE OF POLYMER MATRIX COMPOSITES

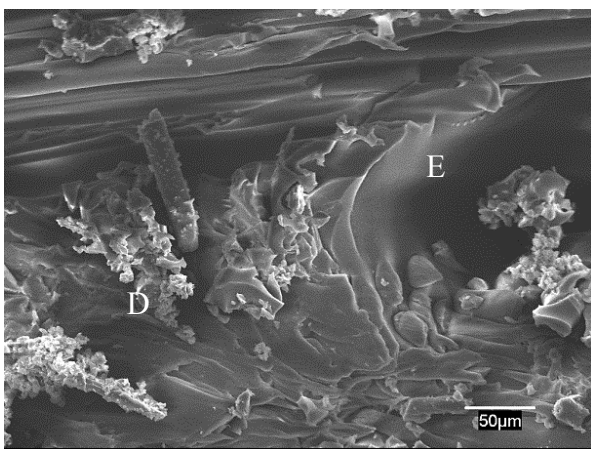
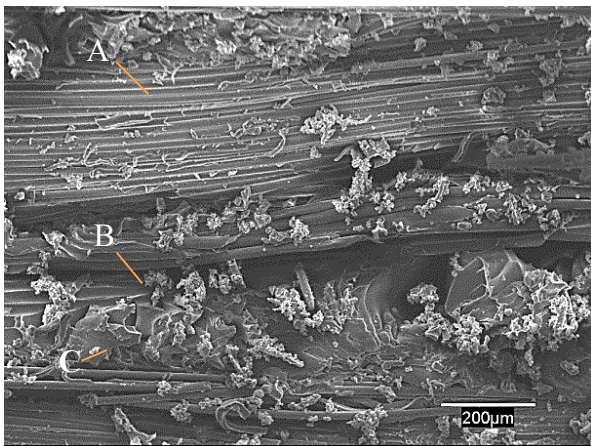


Fig.10.SEM image of the fracture surface
 A. Fibre matrix debonding B. Hackeling C. Fibre pull out D. Matrix stretching and ductile fracture E. void. *debris is left from the SEM sample cutting

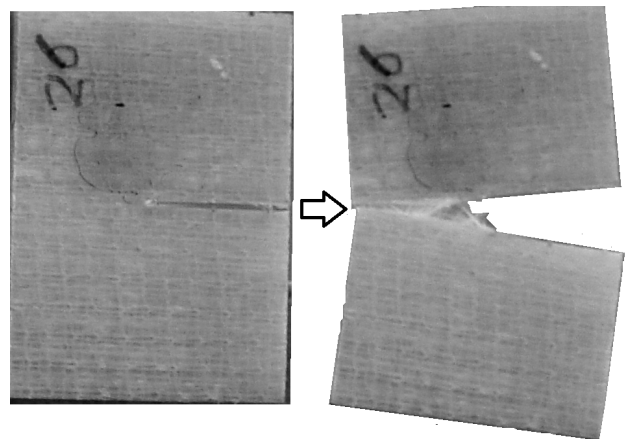
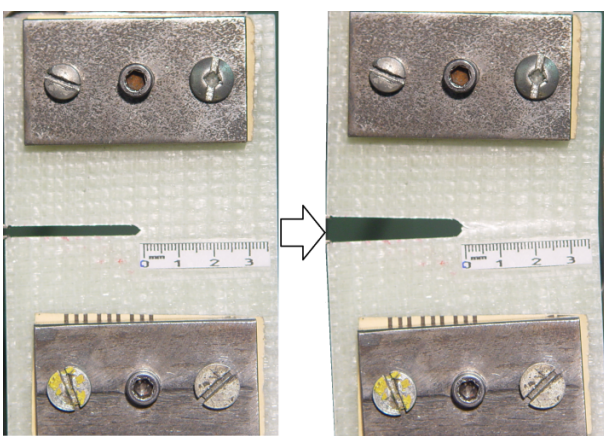


Fig. 11. Hinging effect and rotation at the crack mouth tip.

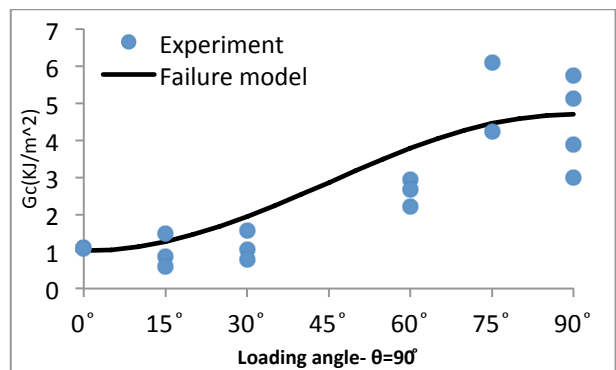


Fig. 12.Comparison of the model prediction and the experiment for 90° UD composite under different modes of loading.

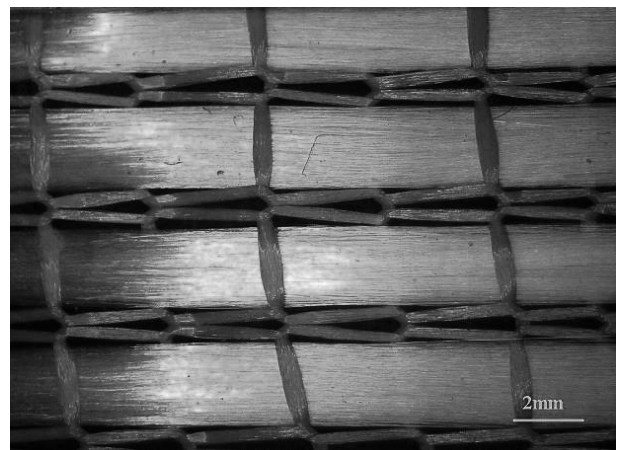


Fig. 13. Periodic threads keeping UD fibres together makes changes in the value of fracture work of the UD composite.

Epoxy(CLR1180/CLH6560 Crosslink)

Mechanical Properties		Unit
E	2.9	GPa
$\sigma_{y.p.}$	30.8	MPa
ν_{12}	0.38[15]	-
UD glass fibre epoxy		
Mechanical Properties		Unit
E1	34.04	GPa
E2	5.032	GPa
E3	5.032	GPa
ν_{21}	0.046*	-
ν_{31}	0.046*	-
ν_{32}	0.35*	-

Table 1: Mechanical properties of epoxy and UD composite used in calculations.

*values are calculated as described in [11].